CFD SIMULATION OF HEAT TRANSFER IN VERTICAL RIBBED TUBE

RABIA ABRAHIM SASI KOSHAD

A thesis submitted in fulfillment of the requirement for the award of the

Degree of Master of Engineering

Faculty of Mechanical and Manufacturing Engineering

University Tun Hussein Onn Malaysia

MAY 2011

ACKNOWLEDGEMENT

I wish to express my thanks to my supervisor; PROF. IR. DR. HJ. ABAS BIN AB WAHAB. This thesis might not have been completed without his expert advice and unfailing patience. I am also most grateful for his faith in this study especially in the sometimes-difficult circumstances. I would like to express a special word of thanks to my friends and family who tirelessly listened to my ideas and offered encouragement when it was most needed A special thanks to my parents for their help I owe everything to them.

ABSTRACT

Computational Fluid Dynamics (CFD) simulation of heat transfer and fluid flow analysis in the turbulent flow regime in a spirally ribbed tube and a smooth tube in vertical orientation are presented in this thesis. The ribbed tube has outside diameter of 25mm, maximum inner diameter of 18.80mm, minimum inner diameter of 17.50mm and helix angle of 60^{o} .The smooth tube has outside diameter of 26.7mm and inner diameter of 18.88mm. Both tubes were uniformly heated by passing an electrical current along the tube with a heated length of 1000mm. The CFD simulation was conducted on a vertical orientation of the steel tubes (rifled and smooth) under six different inlet velocities of 0.893m/s, 1.786m/s, 2.38m/s, 2.976m/s,3.57m/s and 4.166m/s. The objective of this thesis is to determine the heat transfer and pressure drop in both vertical smooth and ribbed tubes. The fluid used is water and the initial temperature is 25^{o}C. The heat flux that for heating the tube is equal to 150KW/m^2. During the CFD simulation analysis it was found that for smooth tube at lower inlet velocity, the temperature increases from 298^{0}K to 307.5^{0}K while the pressure drop between inlet and outlet is equal to 741.34 Pa. At higher inlet velocity, the temperature for smooth tube is found increasing from 298^{0}K to 300^{0}K, with the pressure drop is equal to 9402.44 Pa. For the ribbed tube at lower inlet velocity the temperature is increasing from 298^{0}K to 308.5^{0}K, with the pressure drop is found to be 1655.5 Pa. In the case of a higher inlet velocity, the temperature increase in ribbed tube is increasing from 298^{0}K to 300.4^{0}K, while the pressure drop is equal to 23166.5 Pa. It is clear that the temperature difference between ribbed and smooth tube at lower inlet velocity are equal to 10.19^{0}K and 9.27^{0}K, respectively. While at higher inlet velocity their, temperature difference become 2.2^{0}K, and 1.8^{0}K respectively. At the heat flux equal to 300KW/m2 and inlet velocity equal to 0.893 m/s, the temperature difference

between ribbed and smooth tubes are 21.01^0K and 17.95^0K respectively. This result indicates that the ribbed tube has higher heat transfer efficiency than the smooth tube. The pressure drop in the ribbed tube is also found to be less than that of the smooth tube. This clearly shows that the characteristic of ribbed tube is much better than smooth tube. Thus the ribbed tube is able to enhance the heats transfer capability for fluid flow in the tube.

ABSTRAK

Pengkomputeran dinamik bendalir bagi perpindahan haba dan analisis aliran bendalir pada rejim aliran bergelora melalui tiub berulir dan tiub licin pada orientasi menegak dikaji dalam projek ini. Tiub berulir mempunyai ciri-ciri seperti berdiameter luar 25mm, di samping diameter dalam maksimum dan minimum masing-masing adalah 18.80mm dan 17.50mm, serta sudut helix 60^{o}. Manakala tiub licin pula mempunyai diameter luar 26.7mm dan diameter dalam 18.88mm. Bendalir yang digunakan dalam analisis ini adalah air dengan suhu masukan 25^{o}C. Kedua-dua batang paip tersebut dipanaskan dengan seragam menggunakan pemanas elektrik di sepanjang 1000mm batang paip. Projek ini dilaksanakan dengan tujuan untuk menentukan perpindahan haba dan penurunan tekanan di kedua-dua batang tiub. Simulasi pengkomputeran dinamik bendalir telah dilakukan dengan kedudukan tiub keluli berada dalam orientasi menegak. Simulasi dilaksanakan dalam enam kelajuan masukan yang berbeza berbeza iaitu 0.893m / s, 1.786m / s, 2.38m / s, 2.976m / s, 3.57m / s dan 4.166m / s. Fluks panas sebanyak 150KW/m^2 digunakan untuk memanaskan tiub berkenaan. Melalui simulasi ini, didapati suhu untuk tiub licin pada kelajuan masukan yang rendah meningkat daripada 298^{0}K ke 307.5^{0}K, manakala penurunan tekanan di antara masukan dan keluaran adalah 741.34 Pa. Pada kelajuan masukan yang tinggi pula, suhu meningkat daripada 298^{0}K ke 300^{0}K, manakala penurunan tekanan adalah sebanyak 9402.44 Pa. Selain itu, keputusan untuk tiub berulir pula menunjukkan pada kelajuan masukan yang rendah, suhu meningkat daripada 298K ke 308.5^{0}K, dengan nilai penurunan tekanan adalah 1655.5 Pa. Suhu 298^{0}K turut berubah menjadi lebih tinggi kepada 300.4^{0}K pada kelajuan masukan yang tinggi untuk tiub yang sama, manakala penurunan tekanan memberikan nilai 23166.5 Pa. Secara keseluruhannya, keputusan yang telah diperolehi menunjukkan pada kelajuan masukan yang rendah, perbezaan suhu pada tiub berulir dan tiub licin masing-masing adalah 10.19^{0}K dan 9.27^{0}K. Pada kelajuan masukan yang

tinggi pula, perbezaan suhu untuk tiub yang sama masing-masing adalah 2.2^0K dan 1.8^0K. Keputusan untuk simulasi pada fluks panas 300KW/m^2 dan kelajuan masukan 0.893 m / s menunjukkan perbezaan suhu sebanyak 21.01^0K untuk tiub berulir dan 17.95^0K untuk tiub licin. Secara kesimpulannya, tiub berulir mempunyai kecekapan pemindahan haba yang lebih tinggi berbanding tiub licin. Ini jelas membuktikan bahawa ciri-ciri pada tiub berulir adalah lebih baik berbanding tiub licin seterusnya meningkatkan kebolehan pemindahan haba untuk aliran bendalir dalam tiub.

LIST OF CONTENTS

LIST OF TABLES

LIST OF FIGURES

LIST OF SYMBOLS AND ABBREVIATION

CFD	Computational Fluid Dynamics
K	Kelvin
^{o}C	Degrees Celsius
CHF	Computation Heat Flux
α (^{o})	Helix angle
w	Width
C_p	Specific heat
ρ	Dansity
P	Prssuer
τ_w	Wall Shear Stress
u_τ	Friction Velocity
ν	Kinematic viscosity
U_e	Velocity
Re	Reynolds Number
$\overline{C_f}$	Skin Friction Coefficient
Δp	Pressure Drop
μ	Dynamic Viscosity
k	Thermal Conductivity
u, v, w	Velocity component in(x, y, z) coordinates system
$\bar{u}$	Average velocity
$\acute{u}$	Fluctuating velocity

$\bar{p}$	Average pressure
f	Force component in(x, y, z) coordinates system
Φ	The viscous dissipation term
t	The Time
e	Internal energy of mixture, per unit mass
q	Heat Flux

LIST OF APPENDIXES

CHAPTER 1

CFD SIMULATION OF HEAT TRANSFER IN VERTICAL RIBBED TUBE

1.0 Introduction

The proper designs of the tube inner wall will increase the heat transfer to the flowing water; hence it is one of the main factors for its successful usage in boiler. In order to increase the heat transfer and prevent damage to the inner wall of tube, ribbed tubes are applied instead of the smooth walled tubes. The heat transfer coefficient is one of the most important factors for the successful design and operation of inner tube wall to heat transfer on the flowing water. Analysis and modeling of the inner tube wall for boiler is very important, in order to keep the boiler operation below the critical stages.

In recent years, the high cost of energy and material has results an increased effort for producing more efficient heat exchange equipment. The design procedure of heat exchangers is quite complicated, as it needs exact analysis of heat transfer rate and pressure drop. The major challenge in designing a heat exchanger is to make the equipment compact and achieve a high heat transfer rate using minimum pumping power. The improvement of design techniques for heat transfer augmentation is relevant and important for better performance over several engineering applications. (AG Kanaris et al, 2005).

Critical heat flux (CHF) is the heat flux that be heating the water in boiling by power plants. Thus any increase in the critical heat flux will require more power to increase a higher heat fluxes. That is why a better design of inner wall tube is needed to

keep less a power generation required in heating part of the boiler. The success of the low mass flow vertical tube with variable pressure design depends on the capability of the tube internal geometry to promote cooling of the tube when exposed to high heat flux .Therefore, a lot of advanced cooling techniques have been considered for increasing not only heat transfer but also the CHF in the boiler tube. In particular, the CHF in the forced-convection boiling tubes depends on the wetting condition of the tube inside wall. At a certain percentage of steam quality, the smooth tube walls can no longer be kept completely wetted and the heat transfer is sharply reduced at the unwanted tube wall. It is well known that a swirl flow, which makes the tube wall more wetted, can significantly improve the CHF as well as the heat transfer coefficients in the forced convection boiling tube (Chang Ho Kim et al, 2005).

The experimental studies of the tubes that used in boilers has been confirmed that ribbed tube is better than smooth tube for heat transfer .This is caused by the flow in the ribbed tube will in the form of swirl flow, as result the tube wall more wetted, and significantly improve the CHF as well as the heat transfer coefficients in the forced convection boiling tube can be obtained. In recent years it has been conducting numerous experimental studies to improve the performance of the use of ribbed tubes in the boilers. A number of experiments are performed in rifled tubes with different geometry. These experiments are time consuming and expensive.

An alternative way to reduce the experiments cost is to combine them with CFD and analytical modeling Computational heat transfer flow modeling is one of the great challenges in the classical sciences. As with most problems in Engineering, the interest in the heat transfer augmentation is due to its extreme importance in various industrial applications (P.K.Nagarajan et al, 2009).

Computational Fluid Dynamics (CFD) can be considered an effective tool for estimating the momentum and heat transfer rate in this type of heat exchangers and evaluating their performance. However, the accuracy of the calculations depends on the choice of the most appropriate flow model for (CFD) simulation, (Ranjit Gouda et al, 2008).

Enhanced heat transfer Technology is generally classified as active, passive, and compound heat transfer enhancement technologies, respectively, which combines at

least two heat transfer enhancement methods. The main objective of this study is to model the heat transfer augmentation and friction factor for ribbed tube using CFD, which enable us to find the change of temperature and pressure drop.

1.1 Problem Statement

The problems with smooth tubes for boilers are excessive time taken to transfer heat to water, which leads to increased electrical energy used and also severe damage to the boiler wall. As a result ribbed tube is proposed.

1.2 Objectives of Study

1. To determine the fluid flow characteristics in a vertical positioned tube (smooth and ribbed) by means of Computational Fluid Dynamics (CFD).
2. To determine the heat transfer in a vertical tube (smooth and ribbed) by means of Computational Fluid Dynamics (CFD).
3. To determine the pressure drop in a Vertical tube (smooth and ribbed) by means of Computational Fluid Dynamics (CFD).

1.3 Scope Of Stud

Computational Fluid Dynamics (CFD) will be used to determine the characteristics of fluid flow in the ribbed and smooth tube.

1. Water will be used as the fluid domain in Computational Fluid Dynamics (CFD).

2. Steel tube, (smooth and ribbed) will be analyzed by using Computational Fluid Dynamics (CFD).
3. The analysis by using Computational Fluid Dynamics (CFD) will be conducted with tubes placed vertical.
4. The fluid flow in this analyzed will be single phased.

1.4 Expected Results

At the end of this study, the fluid flow characteristics, pressure drop and heat transfer across a vertical smooth and ribbed tubes will be determined by using Computational Fluid Dynamics (CFD).

1.5 Summary

The CFD simulation analysis will be carried out on a vertical smooth and ribbed tube to determine the fluid flow properties, the heat transfer and pressure drop across the tube in the different models. In this analysis will be the use of water fluid with different inlet velocities, while the heating for the tube by use electrical Current. The temperature difference and the pressure drop in the tube will be determined by the results for both tubes.

CHAPTER 2

LITERATURE REVIEW

2.0 Introduction.

Heat transfer enhancement is the process of improving the performance of a heat transfer system by increasing the heat transfer coefficient. In the past decades, heat transfer enhancement technology has been developed and widely applied to heat exchanger applications; for example, refrigeration, automotives, process industry, chemical industry etc. To date large numbers of attempts have been made to reduce the size and costs of the heat exchangers, (P.K. Nagarajan et al, 2009).

One of the important challenges in the design of heat exchangers is the enhancement of single-phase heat transfer, especially, when heat exchangers have a single-phase fluid flow on one side and a two-phase flow or phase change on the other side. Common examples are condensers, evaporators, boilers, and other such heat exchangers used in various commercial and industrial applications,(AG Kanaris et al,2005).

2.1 Previous Studies

The Critical Heat Flux (CHF) is the heat flux at which boiling crisis occurs and a sudden deterioration of heat transfer rate occurs. Therefore, some efforts have been exerted to expand the regime of nucleate boiling. In this regard, enhancement of the CHF had become an important topic in the area of heat transfer research and a considerable body of related work has been reported in the literature, (Soon Heung Chang et al, 2006).

There are some studies had been conducted on fluid flow and heat transfer in tubes with helical enhancements Publications dealing with theoretical and empirical models will be discussed. The discussion involves some experimental studies as well as analytical studies. (Lixin Cheng et al, 2006), this paper is presented the study of single phase flow heat transfer and friction pressure drop in a spiral internally ribbed tube. The objective of the present study is to experimentally investigate the single-phase flow heat transfer and pressure drop in an internally, spirally ribbed tube with water and kerosene in the turbulent flow regime. The results obtained with the ribbed tube are compared with those of the smooth tube at equal Reynolds number. The enhancement characteristics of the ribbed tube are assessed by comparing the variation of the ratio of the heat flux to the pumping power, with the Reynolds number for both, the spirally ribbed tube and the smooth tube. According to the experimental data, correlations of the heat transfer coefficients and friction factors are, respectively, proposed for the ribbed tube. The ribbed tube has an outside diameter of 22 mm and an inside diameter of 11 mm (an equivalent inside diameter of 11.6 mm) and the smooth tube has an outside diameter of 19 mm and an inside diameter of 15 mm. Both tubes were uniformly heated by passing an electrical current along the tubes with a heated length of 2500 mm. The working fluids are water and kerosene, respectively. The experimental Reynolds number is in the range of 10^4–$5 \cdot 10^4$ for water and is in the range of 10^4–$2.2 \cdot 10^4$ for kerosene. The experimental results of the ribbed tube are compared with those of the smooth tube. The heat transfer coefficients of the ribbed tube are 1.2–1.6 fold greater than those in the smooth tube and the pressure drop in the ribbed tube is also increased by a factor of 1.4–1.7 as compared with those in the smooth tube for water. The

corresponding values for kerosene are 2–2.7 and 1.5–2, respectively. The heat-transfer enhancement characteristics of the ribbed tube are assessed. This tube is especially suitable for augmenting single-phase flow heat transfer of kerosene. Correlations for the heat transfer and the pressure drop for the spirally ribbed tube are proposed, according to the experimental data. (Chang et al,2005), they present in this paper, critical heat flux (CHF) experiments for flow boiling of R-134a were performed to investigate the CHF characteristics of four-head and six-head rifled tubes in comparison with a smooth tube. Both of rifled tubes having different head geometry have the maximum inner diameter of 17.04 mm while the smooth tube has the average inner diameter of 17.04 mm. The experiments were conducted for the vertical orientation under outlet pressures of 13, 16.5, and 23.9 bar, mass fluxes of 285–1300 kg/m2s and inlet sub cooling temperatures of 5–40 _C in the R-134a CHF test loop. The parametric trends of CHF for the tubes show a good agreement with previous understanding. In particular, CHF data of the smooth tube for R-134a were compared with well-known CHF correlations such as Bowring and Katto correlations. The CHF in the rifled tube was enhanced to 40–60% for the CHF in the smooth tube with depending on the rifled geometry and flow parameters such as pressure and mass flux. In relation to the enhancement mechanism, the relative vapor velocity is used to explain the characteristics of the CHF performance in the rifled tube. (Song Kyu et al ,2007), A study of post-dryout heat transfer was performed with a directed heated smooth tube and rifled tubes using vertical R-134a up-flow to investigate the heat transfer characteristics in the post-dryout region. Three types of rifled tube having different rib height and width were used to examine the effects of rib geometry and compare with the smooth tube, using a mass flux of 70–800 kg/m2 s and a pressure of 13–24 bar (corresponding to an approximate water pressure of 80–140 bar). Fig.2.1, (a)–(c) shows the wall temperature distribution between the smooth tube and the rifled tubes at the pressures of 13, 17 and 24 bar. The heat flux of smooth tube could not exceed the heat flux of 130 KW/m^2 to maintain the wall temperature below 500^oC for prevention of tube damage. Wall temperature distribution in all tubes was strongly dependent on pressure and mass flux. Wall temperatures of the rifled tubes in the post-dryout region were much lower than for the smooth tube at same

conditions. This was attributed to swirl flow caused by the rib. Thus, the thermal non-equilibrium, which is usually present in the post-dryout region, was lowered.

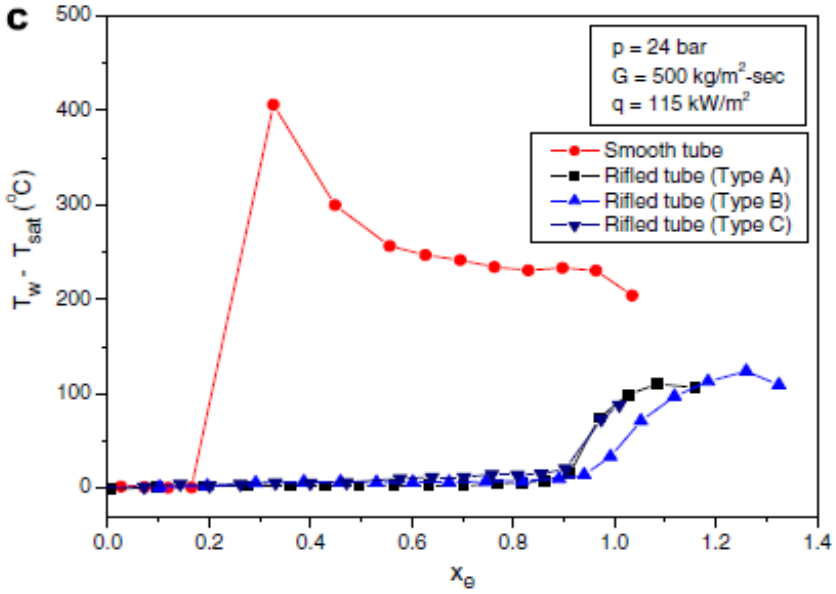

Fig.2.1. Wall temperature distribution in a smooth tube and three rifled tubes at (a)13, (b) 17 and (c) 24 bar. (Song Kyu et al, 2007).

The empirical correlation of heat transfer in the smooth tube of the post-dryout region was obtained. The heat transfer correlation for rifled tubes was also obtained as a function of rib height and width with the modification of the smooth tube correlation. (Dragan R. Tucakovic et al,2006), this paper presents a methodology and results of detailed thermal–hydraulic simulations and analyses of the forced circulation loop of the large steam boiler in the Thermal Power Plant. The rifled tubes in the furnace zone of the evaporating tubes are considered. Calculations are performed for the load range from 40% to 100% of the full power. A dependence of all important thermal and hydraulic parameters in the evaporating tubes on the boiler load is predicted, such as working fluid flow rate, steam void fraction, circulation number, circulation velocity, and critical heat flux along the evaporating tubes. In order to demonstrate the influence of the rifled tubes on the increase of the evaporating tubes thermal margin against the burnout and on the circulation loop friction pressure drop, comparative calculations with evaporating smooth tubes are performed. Also, a range of lower loads for which

the natural circulation is acceptable is predicted. On the basis of obtained analytical results, the relation between the circulation number and the steam production is derived. The conducted analyses show that the rifled tubes prevent the critical heat transfer conditions in the furnace zone under all operating conditions and under supposed non-uniform heat load distribution among the evaporator's walls. In case of non-uniform heat load the critical heat flux can be reached in the convective zone of the most loaded evaporating tubes. But, in this zone the heat fluxes are lower compared to the furnace zone and they cannot lead to the tubes burnout. In case of the smooth tubes application in the evaporator furnace zone, shows that the critical heat transfer conditions can be reached in the furnace zone under non-uniform heat load distribution among the evaporating walls. The conducted analyses show that the rifled tubes prevent the critical heat transfer conditions in the furnace zone under all operating conditions and under supposed non-uniform heat load distribution among the evaporator's walls. In case of non-uniform heat load the critical heat flux can be reached in the convective zone of the most loaded evaporating tubes. But, in this zone the heat fluxes are lower compared to the furnace zone and they cannot lead to the tubes burnout. In case of the smooth tubes application in the evaporator furnace zone that the critical heat transfer conditions can be reached in the furnace zone under non-uniform heat load distribution among the evaporating walls. This fact justifies the need for the rifled tubes implementation in the furnace zone of the evaporator. (Van Duijn, 2006), investigated the process of the bubble growth and detachment from a wall with uniform up flow parallel to the wall. He have been designed and performed in such a way that the assumptions of an existing analytical model were met. The aim of this study was to validate the predictions and to quantify the hydrodynamic lift force on a boiling bubble. This kind of detailed modeling of detachment can in principle be combined with numerical modeling of flow with heat transfer in evaporator tubes, rifled tubes, with the aid of commercially available packages. The findings can be used to predict boiling characteristics in complicated geometries, such as rifled tubes, for conditions that occur during deferent operation regimes of conventionally fired power plants. Used in this study ribbed and smooth tube. A way to overcome this problem is to create swirl in vertical tubes with up flow by introducing rifled evaporator tubes. Producers of rifled tubes base design

recommendations for evaporators on experiments. Producers of rifled tubes base design recommendations for evaporators on experiments, see Fig. 2.2. The performance of the so-called rifled tubes is much better than the performance of the smooth evaporator tubes.

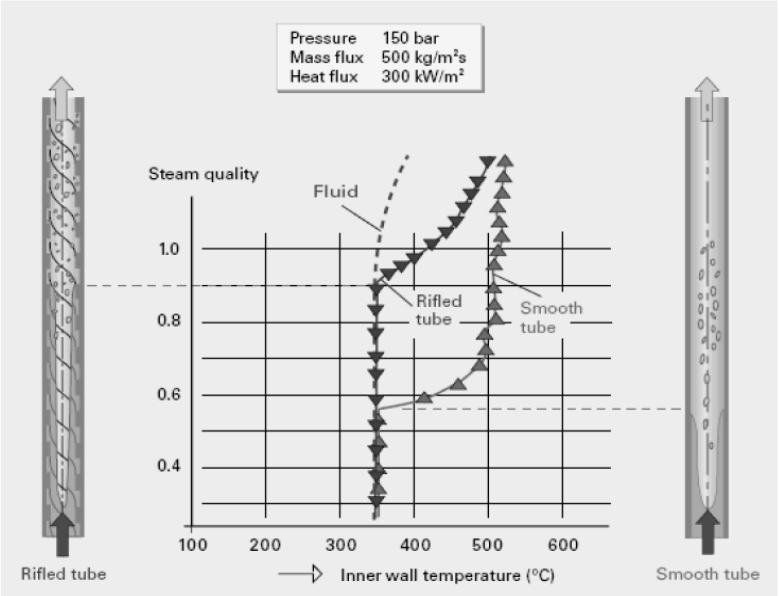

Figure 2.2 Improvement in heat transfer by rifled tubes: Wall temperature in smooth and rifled tubes, (Van Duijn, 2006).

A number of experiments is per- formed in rifled tubes with different geometry to increase their performance. The advantage of a rifled evaporator tube is the presence of mechanisms that move bubbles, formed at the inner wall, towards the center. An additional body force, induced by the swirling motion created by fluid flowing along helically shaped ribs .(P.K. Nagarajan el at,2009), The main objective of this study is to model the heat transfer augmentation and friction factor characteristics for the circular tube fitted with right-left helical twist insert with 100 mm spacer using CFD, which enable us to find out Nusselt number. The CFD simulation for the heat transfer augmentation in a circular tube fitted with right-left helical inserts with 100 mm spacer in laminar flow conditions has been explained in this paper using Fluent version 6.2.16. The data obtained by simulation are matching with the literature value for plain tube with the discrepancy of less than, $\mp$ 5%, for Nusselt number and friction factor.

Enhanced heat transfer with decreasing twist ratio has been observed. Heat flux is more uniform all along the tube and decreases uniformly towards the center. Right-left movement of the flow as per direction twist was also observed from the velocity contour. (Gregory Zdaniuk, 2006), he was study in this paper the heat transfer and friction in helically-find tubes using artificial neural networks. This dissertation first introduced heat transfer enhancements techniques. A literature review of heat transfer and friction in tubes with helical enhancements (indentations, ribs, fins, wire inserts, or spiral tapes) was performed, and available prediction methods were reported. The current understanding of complex secondary flows in the interim region was discussed. An introduction to artificial neural networks (ANNs) was presented, and a literature review of the use of (ANNs) in heat transfer and fluid flow was conducted. Next, heat transfer coefficients and friction factors were determined experimentally for eight helically-finned tubes and one smooth tube using liquid water at 12 000 < *Rei* < 60 000. An uncertainty analysis was completed and plain-tube results were compared to the Blasius and Dittus-Boelter equations with satisfactory agreement.

CHAPTER 3

STUDY METHODOLOGY

3.0 Computational Domain

The commercial CFD code FLUENT (FLUENT, 6.3.26) will be used to analyze the model flow characteristics of smooth and ribbed tube. Modeling and mesh generation are however performed in Gambit environment. Water will be taken as the fluid medium. Figure 3.1 show the schematic diagram of the ribbed tube model that comprises a 25mm outer diameter, 18.8mm maximum inlet diameter and 17.5mm minimum inlet diameter. The length of the tube 1m, the rib height is 0.6835mm and the width is 9.25mm.The helix angle is 60^{o}, and the number of starts is 4. The ribbed tube parameter used in this analysis is show in table 3.1. The flow chart for CFD works study shown in figure A5, appendix A.

Table 3.1 the dimension of the ribbed tube geometry parameter.

Tube type	Outer diameter, OD (mm)	Maximum inner diameter, ID_{max} (mm)	Minimum inner diameter, ID_{min} (mm)	Rib height, t (mm)	Rib width, w (mm)	Helix angle, α (^{o})	Number of starts
Steel	25.00	18.80	17.50	0.6835	9.25	60	4

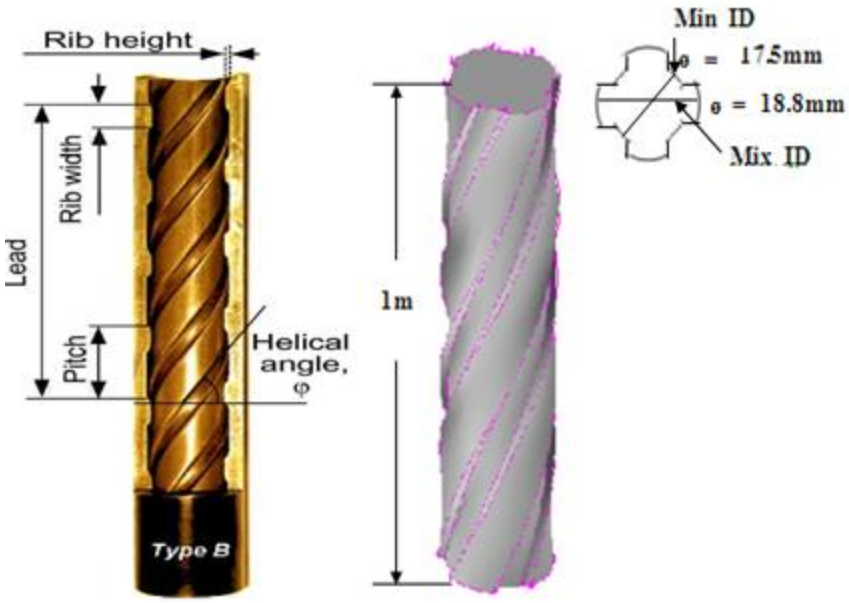

Figure 3.1 Schematic diagram of a ribbed tube (Chang et al, 2005).

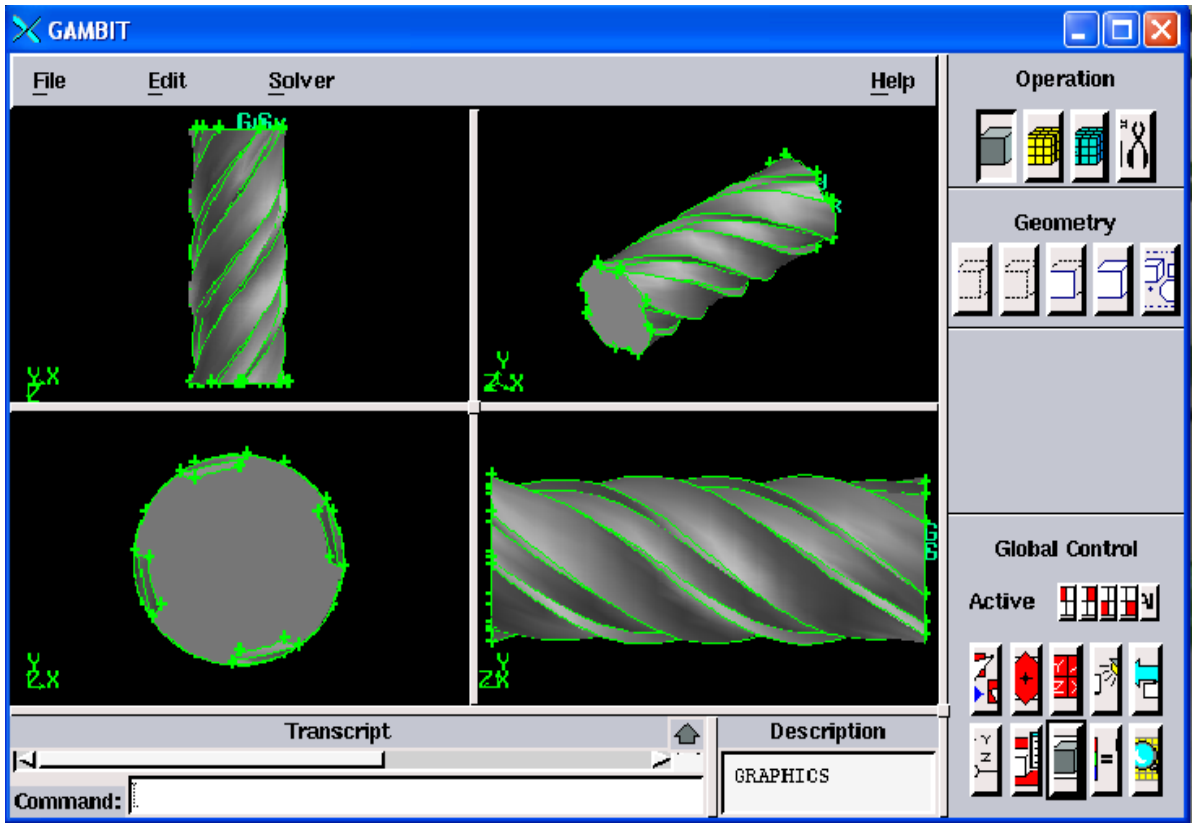

Figure 3.2 show the drawing for ribbed tube in the Gambit.

The schematic diagram of the smooth tube model show in figure 3.3, that comprise an outer diameter is 26.7mm, Inner diameter is 18.88mm, the wall thickness is 3.91mm, and the length of smooth tube is 1m. The smooth tube parameter used in this analysis is show in table3. 2.

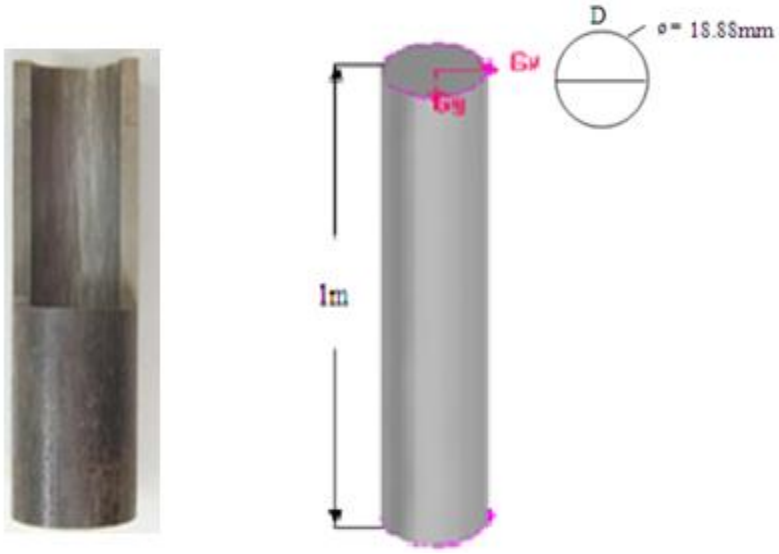

Figure 3.3 Schematic diagram of a smooth tube.

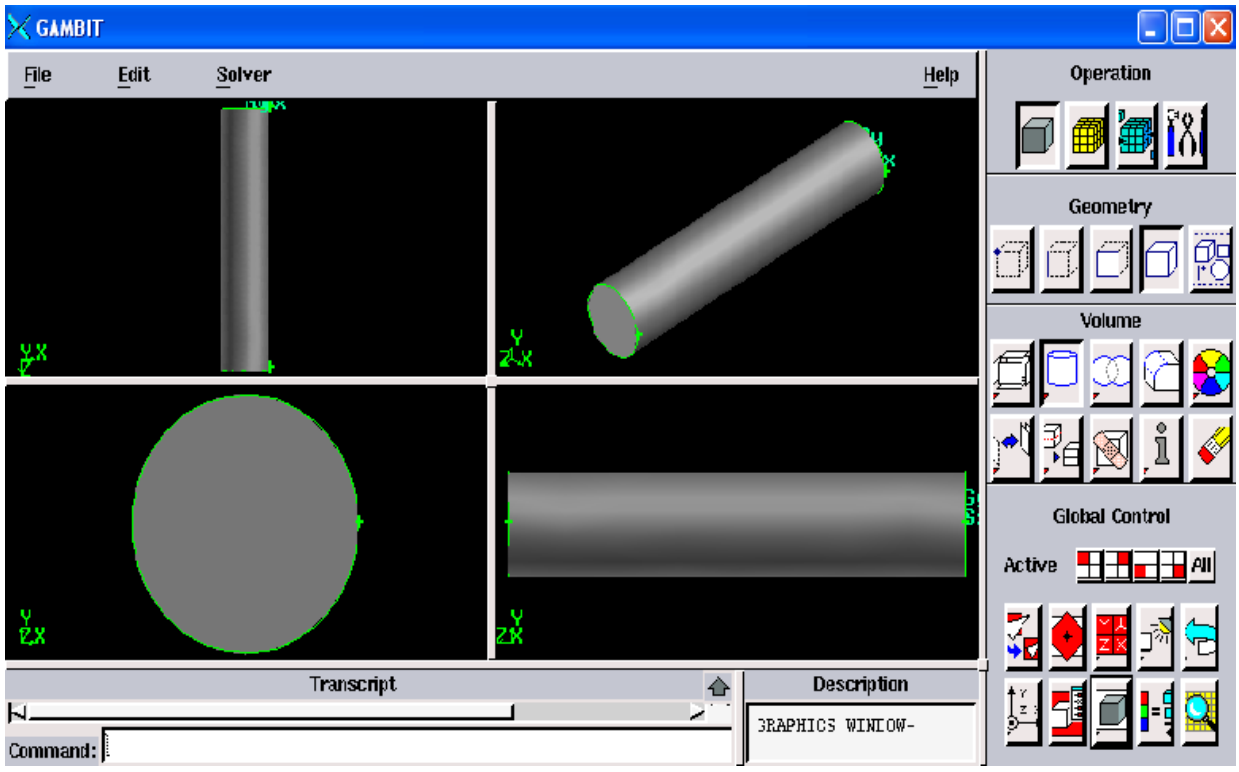

Figure 3.4 show the drawing for the smooth tube in Gambit.

Table 3.2 the dimension of the smooth tube geometry parameter.

Tube type	Outer diameter OD (mm)	Wall Thickness w(mm)	Inner diameter ID (mm)
Steel	26.7	3.91	18.88

3.1 Boundary Conditions

The present work set both the tubes is sited vertically and the flow inside the tube is assumed as fully turbulent flow. The water temperature is set at 25^{o}C (298^{o} K), with water properties at that temperature as shown in the table 3.3. Figure 3.5 shows the prescribed boundary condition for solving this flow problem numerically by using Fluent software. In that figure, q is representing the heat flux at constant rate which created by passing an electrical current (150 KW/m^2) along 1 meter tube length. At the inlet station, the water velocity can be set for different value. The present study carries out six different inlet velocities at constant inlet temperature 25^{o}C. Those six inlet velocities are: 0.893, 1.786, 2.38, 2.976, 3.57 and 4.166 m/s.

Table 3.3 the properties of water at temperature at (298^{o} K).

Temperature *(K)*	Density ρ (kg/m^3)	Specific heat *Cp (j/kg.K)*	Thermal conductivity *k(w/m.k)*	Dynamic Viscosity μ*(kg/m.s)*
298	997.1	4180	0.6055	0.000891

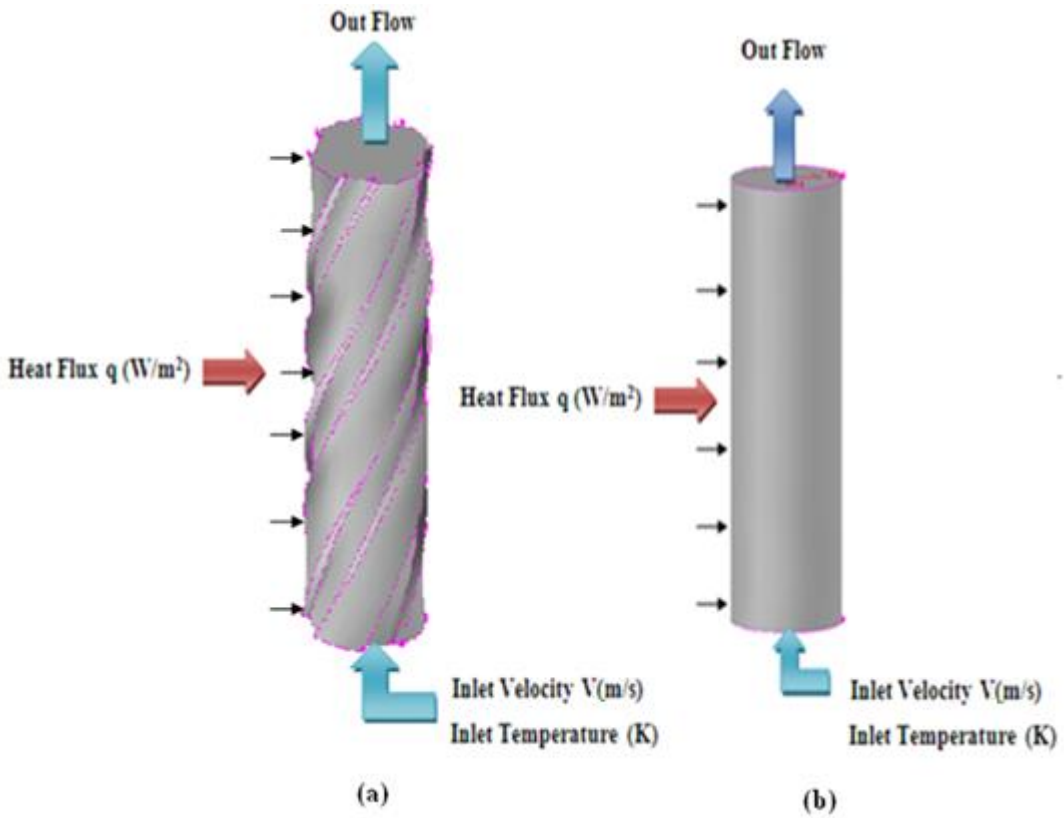

Figure3.5 Boundary conditions, (a) ribbed tube, (b) smooth tube.

The tube uses a steel material and it had been found the material properties are a constant if the steel operated below 300^{o} K and they will vary if the temperature above of it. The steel properties in term of density ρ , the specific heat coefficient at constant pressure C_p and thermal conductivity k below 300^{o} K are shown in the Table. 3.4.

Table 3.4.The properties of Steel at (300^{0} K).

Type of tube	Density ρ (kg/m^3)	Specific heat C_p $(j/kg.K)$	Thermal conductivity k $(w/m.K)$
Steel	8030	502.48	16.27

3.2 Governing Equations

As the fluid medium as water and the flow velocity is relative low and steady, so the flow problem in hand can be considered as incompressible steady flow problem. In assumption that water behave as a Newtonian fluid, the governing equation of the flow problem in hand written in the Cartesian coordinate system as: (Klaus et al, 1996).

Continuity Equation:

$$\frac{\partial u}{\partial x}+\frac{\partial v}{\partial y}+\frac{\partial w}{\partial z}=0 \tag{3.1}$$

The momentum equation in three space direction as:

x –component

$$\rho\left(\frac{\partial u}{\partial t}+u\frac{\partial u}{\partial x}+v\frac{\partial u}{\partial y}+w\frac{\partial u}{\partial z}\right)=\rho f_x-\frac{\partial p}{\partial x}+\mu\left(\frac{\partial^2 u}{\partial x^2}+\frac{\partial^2 u}{\partial y^2}+\frac{\partial^2 u}{\partial z^2}\right) \tag{3.2}$$

y -component

$$\rho\left(\frac{\partial v}{\partial t}+u\frac{\partial v}{\partial x}+v\frac{\partial v}{\partial y}+w\frac{\partial v}{\partial z}\right)=\rho f_y-\frac{\partial p}{\partial y}+\mu\left(\frac{\partial^2 v}{\partial x^2}+\frac{\partial^2 v}{\partial y^2}+\frac{\partial^2 v}{\partial z^2}\right) \tag{3.3}$$

z -component

$$\rho\left(\frac{\partial w}{\partial t}+u\frac{\partial w}{\partial x}+v\frac{\partial w}{\partial y}+w\frac{\partial w}{\partial z}\right)=\rho f_z-\frac{\partial p}{\partial x}+\mu\left(\frac{\partial^2 w}{\partial x^2}+\frac{\partial^2 w}{\partial y^2}+\frac{\partial^2 w}{\partial z^2}\right) \tag{3.4}$$

The system equation as given by Eq. 3.2 to 3.4 represents the governing equation of laminar flow. The turbulent flow equation can be obtained by presenting the

all flow variables in above system consists of average and fluctuated value, for instance the component velocity in *x* direction u becomes:

$$u(x,y,z,t) = \bar{u}(x,y,z,t) + u'(x,y,z,t) \tag{3.5}$$

Putting such relationship as given by eq. 3.5 into the laminar Navier Stokes equation and take averaging process, one will obtain the momentum equation in the form as :(K Muralidhar et al, 2005).

$$\rho\left[\frac{\partial\bar{u}}{\partial t} + \bar{u}\frac{\partial\bar{u}}{\partial x} + \bar{v}\frac{\partial\bar{u}}{\partial y} + \bar{w}\frac{\partial\bar{u}}{\partial z}\right] = -\frac{\partial\bar{p}}{\partial x} + \mu\nabla^2\bar{u} - \rho\left[\frac{\partial}{\partial x}\overline{u'^2} + \frac{\partial}{\partial y}\overline{u'v'} + \frac{\partial}{\partial z}\overline{u'w'}\right] \tag{3.6}$$

In above equation contain the term $\rho u'v'$ which is known shear Reynolds stress term. Such term need to be modeled if the Time averaged Navier Stokes to be solved. The present work use Fluent with K-$\mathcal{E}$ turbulence modeling.

3.3 Conservation of Energy

The modified form of the first law of thermodynamics applied to an element of fluid states that the rate of change in the total energy (intrinsic plus kinetic) of the fluid as it flows is equal to the sum of the rate at which work is being done on the fluid by external forces and the rate on which heat is being added by conduction, (P.K. Nagarajan et al, 2009).The energy equation with heat generation, Fourier heat conduction Newtonian fluid Stokes hypothesis is,(Klaus et al,1996).

$$\rho\left(\frac{\partial e}{\partial t} + u\frac{\partial e}{\partial x} + v\frac{\partial e}{\partial y} + w\frac{\partial e}{\partial z}\right) + \frac{\partial q}{\partial t} = \frac{\partial}{\partial x}\left(k\frac{\partial T}{\partial x}\right) + \frac{\partial}{\partial y}\left(k\frac{\partial T}{\partial y}\right) + \frac{\partial}{\partial z}\left(k\frac{\partial T}{\partial z}\right) - p\left(\frac{\partial u}{\partial x} + \frac{\partial v}{\partial y} + \frac{\partial w}{\partial z}\right) + \Phi \tag{3.7}$$

Where Φis known as the viscous dissipation term:

$$\Phi = \left\{2\left[\left(\frac{\partial u}{\partial x}\right)^2 + \left(\frac{\partial v}{\partial y}\right)^2 + \left(\frac{\partial w}{\partial z}\right)^2\right] + \left(\frac{\partial u}{\partial y} + \frac{\partial v}{\partial x}\right)^2 + \left(\frac{\partial w}{\partial y} + \frac{\partial v}{\partial z}\right)^2 + \left(\frac{\partial u}{\partial z} + \frac{\partial w}{\partial x}\right)^2 - \frac{2}{3}\left(\frac{\partial u}{\partial x} + \frac{\partial v}{\partial y} + \frac{\partial w}{\partial z}\right)^2\right\} \quad (3.8)$$

3.4 Grid Independence Study

Turbulent flows are significantly affected by the presence of walls, as these are the main source of mean vorticity and turbulence .Therefore the available tool in FLUENT, the standard wall functions are used for the near-wall treatments, where the laws-of-the-wall for mean velocity are based on the wall unit, y^+.

For standard wall functions, each wall-adjacent cell's centroid should be located within the log-law layer (figure 3.4).

$$y_p^+ \approx 30 - 300 \quad (3.9)$$

How to estimate the size of wall-adjacent cells before creating the grid:

$$y_p^+ \equiv y_p u_\tau / \nu \Rightarrow y_p \equiv y_p^+ \nu / u_\tau \quad , \quad u_\tau \equiv \sqrt{\tau_w / \rho} = U_e \sqrt{\overline{C}_f / 2} \quad (3.10)$$

Where:

τ_w is the Wall Shear Stress ($kg.s^{-2}.m^{-1}$)

u_τ is the Friction Velocity ($u_\tau = (\tau_w/\rho)^{1/2}$) ($m.s^{-1}$)

ρ is the Density (kg.m−3)

ν is the Kinematic viscosity ($m^2.s^{-1}$)

U_e is the velocity (m/s)

The skin friction coefficient ($\overline{C_f}$) for duct can be estimated from empirical correlations: :(www.Fluentusers.com)

$$\frac{\overline{C}_f}{2} \approx 0.039\,\mathrm{Re}_D^{-1/4} \qquad (3.11)$$

Applying the most recommended non-dimensional distance from the wall, y^+≈60-80 gives the finest mesh to be 1.1 mm. Finer mesh is not to be expected to lead to accurate results. Therefore a grid independence study was carried out for three mesh interval sizes of 1.1mm, 1.2mm and 1.3mm which generate approximately 198380,167400 and 127755 mesh volumes respectively for the empty plenum, figure3.6.

Fig 3.6, show the result of pressure profiles for various mesh sizes. Overlap with each other the result will not change for further mesh refinement the result is grid independent 1.1mm.

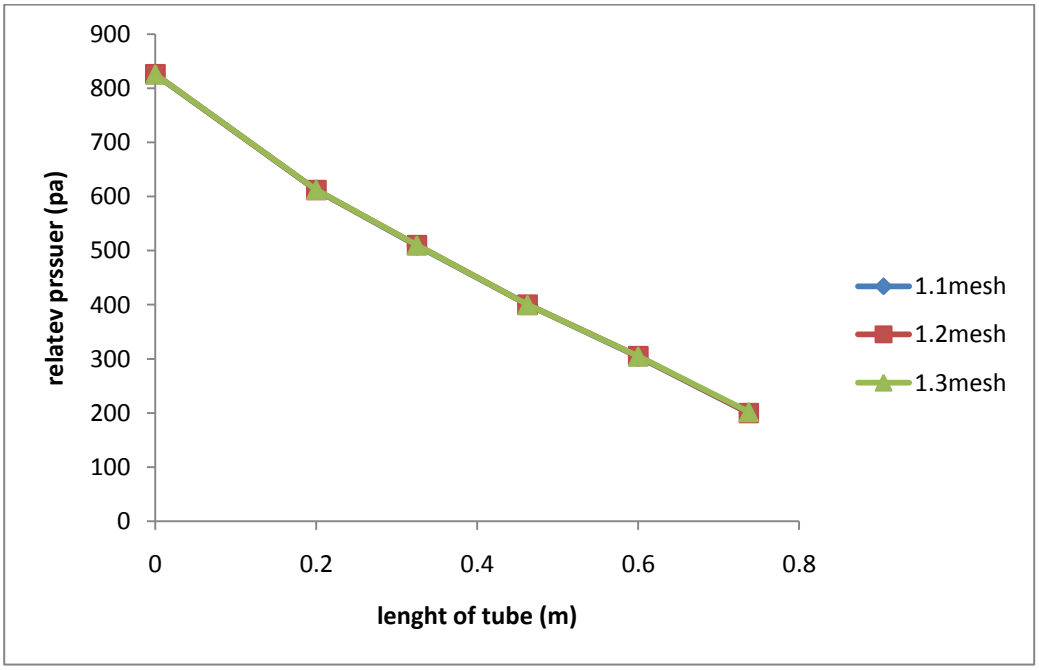

Figure 3.6 pressure profiles for various mesh sizes (mm).

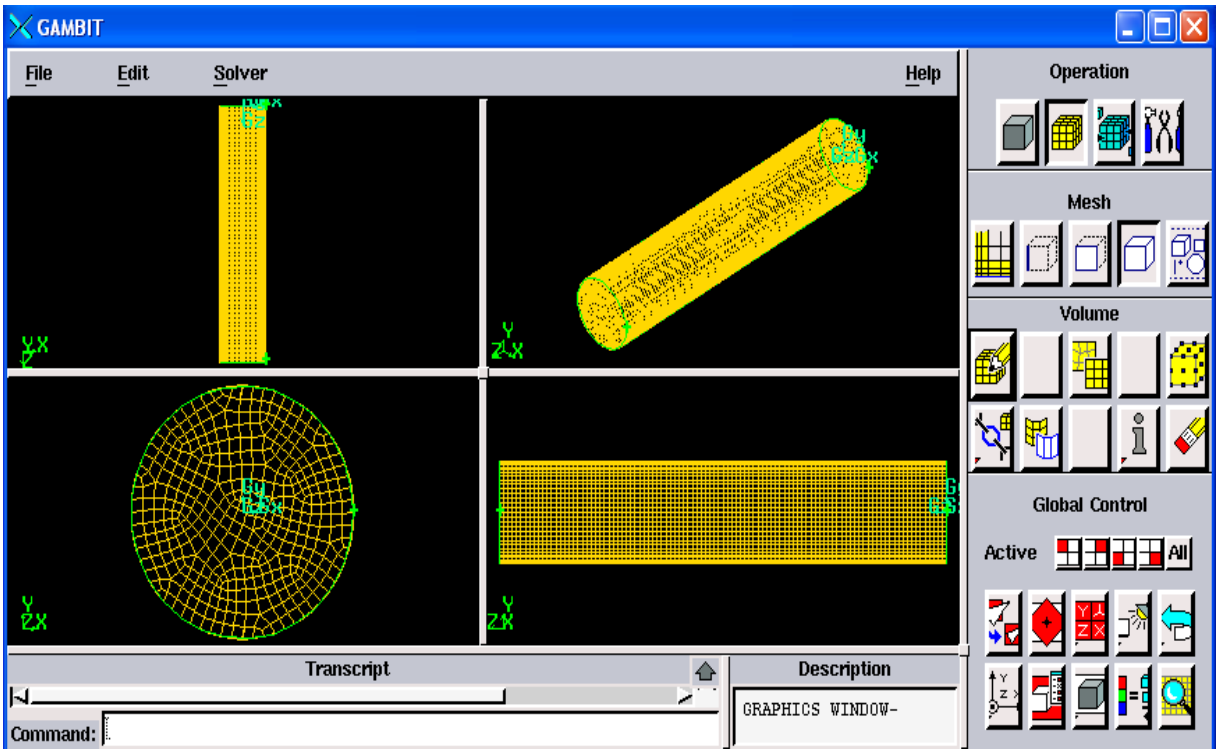

Figure 3.7 Show the mesh in Gambit of smooth tube.

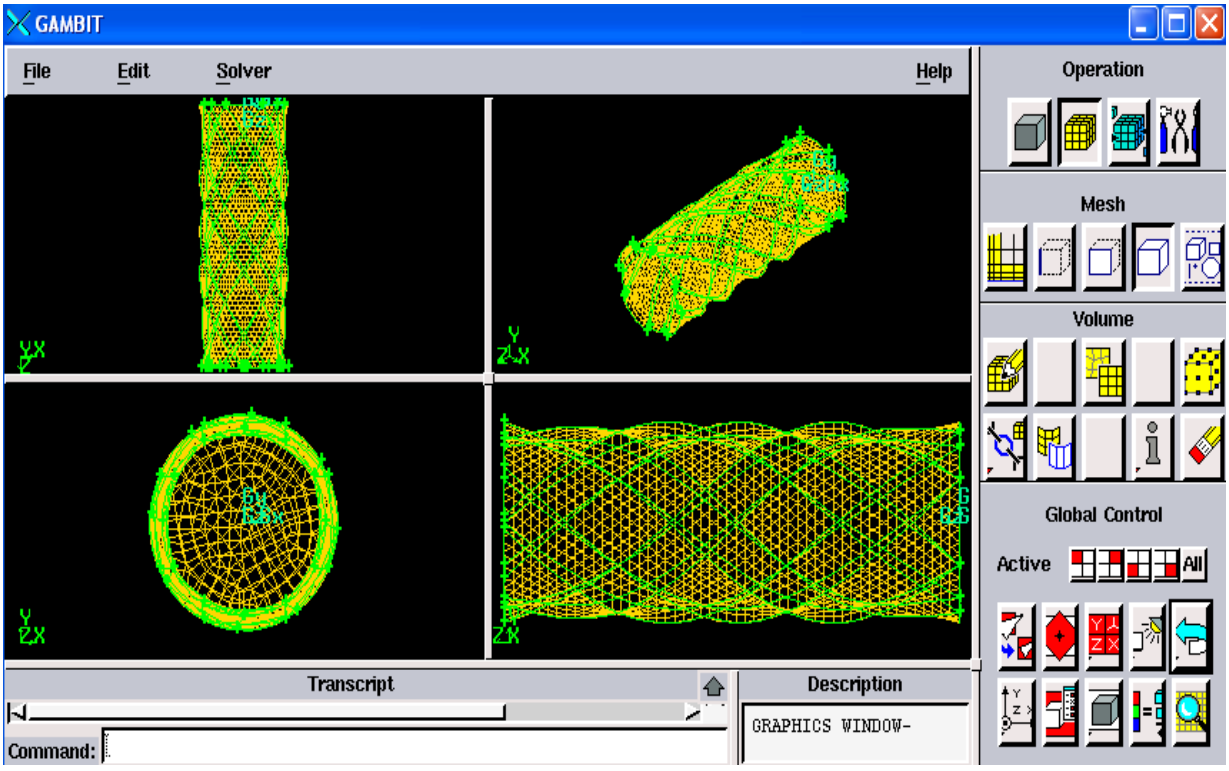

Figure 3.8 Show the mesh in Gambit of ribbed tube.

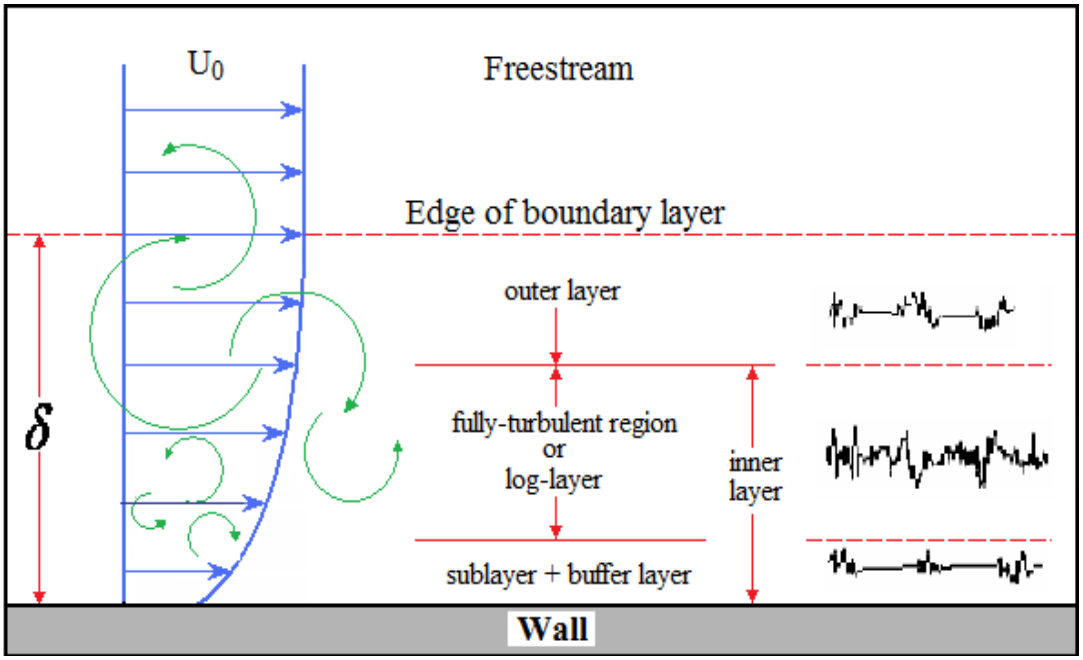

Figure 3.9 the structure of turbulent boundary layers in the near-wall region.

3.5 Pressure Drop

Low pressure drop across tube is another desired characteristic of the tube as it leads to less pumping power needed for the system to work. While extracting the pressure drop from the numerical results, the following equation applies:

$$\Delta p = p_1 - p_2 \tag{3.12}$$

Where, p_1 and p_2 are the average static pressure at the inlet and outlet (actual) surfaces respectively.

CHAPTER 4

RESULTS AND DISCUSSION

4.0 Introduction

The CFD analysis studies by use of fluent software for the flow along the tube with heat transfer effects are presented. The CFD analysis applied for the case of internal flow problems through a vertically positioned smooth and ribbed tube in order to determine the heat transfer and pressure drop along the tube. Comparison result among of them will be carried out to determine the most suitable tube model in handling the heat transfer problem.

4.1 Fixed Heat Flux with Different Inlet Velocities

4.1.1 Simulation Results for Smooth Tube

CFD simulation study was carried out using the smooth tube with six different inlet velocities at constant temperature ($25^{o}C$) and heat flux (150 KW/m^2). The result of

temperature along the tube were outed six different positions starting from the inlet position as x = 0 to the out let position as x = 1. The temperature distribution for different inlet conditions are shown in the Table, 4.1. Figure 4.1 shows these distribution graphically . The total temperature distribution along tube is shown in figure A1, appendix A.

Table 4.1 Temperature distribution along smooth tube for six different inlet velocities.

Length of tube (m)	T (K) at 0.893 m/s	T (K) at 1.786 m/s	T (K) at 2.38 m/s	T (K) at 2.976 m/s	T (K) at 3.57m/s	T (K) at 4.166 m/s
0	298.23	298.2	298.197	298.19	298.19	298.19
0.2	299.025	298.485	298.347	298.263	298.208	298.168
0.4	299.965	298.9	298.657	298.51	298.412	298.342
0.6	301.444	299.485	299.056	298.816	298.657	298.559
0.8	303.111	300.257	299.611	299.247	298.999	298.844
1	307.5	303	301	301	300.5	300

It is clear from figure 4.1 that the temperatures along the tube increased for all cases, but the highest temperature increment occurs at the small inlet velocity. At the inlet velocity equals to 0.893 m/s, the temperature rises from 298^0 K to 307.5^0 K , while at a higher inlet velocity, namely at velocity 4.166 m/s, the temperature increment is only 1 degree is from, 298^0 K, to 300^0 K . This result indicates that a lower inlet velocity is better than a higher inlet velocity.